Inhibition of cell membrane ingression at the division site by cell walls in fission yeast

Ting Gang Chew[a,b,†], Tzer Chyn Lim[a,†], Yumi Osaki[c], Junqi Huang[a], Anton Kamnev[a], Tomoyuki Hatano[a], Masako Osumi[c,d], and Mohan K. Balasubramanian[a,*]
[a]Division of Biomedical Sciences, Warwick Medical School, University of Warwick, Coventry, CV4 7AL, United Kingdom; [b]ZJU-UoE Institute, Zhejiang University School of Medicine, International Campus, Zhejiang University, Zhejiang 314400, People's Republic of China; [c]Integrated Imaging Research Support, Tokyo 102-0093, Japan; [d]Laboratory of Electron Microscopy/Bio-imaging Center, Japan Women's University, Tokyo 112-8681, Japan

ABSTRACT Eukaryotic cells assemble actomyosin rings during cytokinesis to function as force-generating machines to drive membrane invagination and to counteract the intracellular pressure and the cell surface tension. How the extracellular matrix affects actomyosin ring contraction has not been fully explored. While studying the *Schizosaccharomyces pombe* 1,3-β-glucan-synthase mutant *cps1*-191, which is defective in division septum synthesis and arrests with a stable actomyosin ring, we found that weakening of the extracellular glycan matrix caused the generated spheroplasts to divide under the nonpermissive condition. This nonmedial slow division was dependent on a functional actomyosin ring and vesicular trafficking, but independent of normal septum synthesis. Interestingly, the high intracellular turgor pressure appears to play a minimal role in inhibiting ring contraction in the absence of cell wall remodeling in *cps1*-191 mutants, as decreasing the turgor pressure alone did not enable spheroplast division. We propose that during cytokinesis, the extracellular glycan matrix restricts actomyosin ring contraction and membrane ingression, and remodeling of the extracellular components through division septum synthesis relieves the inhibition and facilitates actomyosin ring contraction.

INTRODUCTION

Animal cells and fungal cells require assembly and contraction of an actomyosin ring during cytokinesis. In fission yeast, the actomyosin ring contracts to drive membrane ingression and coordinates with the septum assembly machinery to deposit cell wall materials at the division site (Ramos *et al.*, 2019). The fungal cell wall has been suggested to be a functional equivalent of the extracellular matrix (ECM) in animal cells (Munoz *et al.*, 2013). The division septum is a special wall structure composed of primary and secondary septa. The primary septum is a structure that must be degraded to permit cell separation and the secondary septum is a structure that forms the cell wall once the cells are separated. The septum assembly machinery consists of α-glucan synthase Ags1 and β-glucan synthase Bgs1 and Bgs4. The β-glucan synthase Cps1/Bgs1 is essential for primary septum formation. Cps1 synthesizes specifically the linear β-glucan matrix of the primary septum at the division site and couples the extracellular glycan matrix to the actomyosin ring via intermediate protein complexes (Munoz *et al.*, 2013; Cortes *et al.*, 2015; Davidson *et al.*, 2016; Sethi *et al.*, 2016). The β-glucan synthases Bgs4 and the α-glucan synthase Ags1 are primarily involved in the secondary septum formation and participate in the synthesis of primary septum (Garcia Cortes *et al.*, 2016). The deposition of extracellular glycan matrix coordinates with actomyosin ring contraction and stabilizes the contracting actomyosin ring at the division site (Munoz *et al.*, 2013; Arasada and Pollard, 2014).

How the extracellular glycan matrix influences actomyosin ring contraction (apart from its roles in ring stability during cytokinesis) has not been examined closely (Mishra *et al.*, 2012; Munoz *et al.*, 2013). In this study, we used the thermosensitive allele of

β-1,3-glucan synthase, cps1-191, to address this question. The cps1-191 mutant is defective in β-1,3-glucan and septum synthesis and arrests with a noncontracting actomyosin ring at the nonpermissive temperature (Liu et al., 2000). Interestingly, we found that weakening of the extracellular glycan matrix in cps1-191 mutant at the nonpermissive temperature enabled actomyosin ring contraction and membrane ingression.

RESULTS AND DISCUSSION

At the restrictive temperature, the β-glucan synthase mutant cps1-191 assembles actomyosin rings that do not contract (Liu et al., 2000). It has been suggested that β-glucan synthesis at the division site is required to overcome the high intracellular turgor pressure during cytokinesis, and that the actomyosin ring may not be able to overcome the high turgor (Proctor et al., 2012). To test if the turgor pressure inhibited ring contraction in cps1-191 mutants, we cultured cps1-191 cells in EMMA medium containing 0.8 M sorbitol to decrease the turgor pressure to that inside the cells at the restrictive temperature, and we added 2-deoxyglucose (2-DG) to this culture to prevent further glucan synthesis at the division site and elsewhere in the cells (Megnet, 1965; Svoboda and Smith, 1972; Osumi et al., 1998). A recent study showed that rings in cps1-191 mutant cells constricted slowly after shifting to the restrictive temperature for ~2 h before microscopy at the restrictive temperature (Dundon and Pollard, 2020). To ensure a highly penetrant phenotype for cps1-191, we shifted the cps1-191 cells to the restrictive temperature for ~6 h before microscopy, which was performed at the restrictive temperature. As previously reported, actomyosin rings of cps1-191 cells maintained at normal turgor pressure did not undergo contraction (Figure 1A). We occasionally observed that parts of the cps1-191 cells swelled into bumps and the cells lysed eventually with collapsing rings (Figure 1B). Culturing cps1-191 cells in EMMA medium containing 0.8 M sorbitol did not increase actomyosin ring contraction events, and phenotypically these cells resembled cps1-191 grown under normal growth conditions in EMMA medium, in which a high intracellular turgor pressure is maintained (Figure 1, C and D). Thus, our results showed that a decreased turgor pressure does not allow ring contraction in cps1-191 mutant cells.

Next, we considered the possibility that the extracellular glycan matrix inhibited ring contraction and membrane ingression in cps1-191 mutants in the absence of cell wall remodeling. The Cps1 is a transmembrane protein that (along with other integral membrane proteins, such as Ags1 and Bgs4) links actomyosin rings underneath the cell membrane to the extracellular glycan matrix (Cortes et al., 2005, 2012; Munoz et al., 2013; Arasada and Pollard, 2015; Davidson et al., 2016; Sethi et al., 2016; Martin-Garcia et al., 2018). It was possible that in the absence of division septum synthesis (and thus cell wall remodeling), the actomyosin rings were stably fixed to the inactive cps1-191 gene product or other integral membrane proteins (such as mok1, sbg1, and bgs4) that link the cell wall to the actomyosin ring. To test if this was the case, we weakened the extracellular glycan matrix by treating the cps1-191 cells with cell wall–lytic enzymes and further blocking new cell wall and septum synthesis by supplementing the culture with 2-DG. Interestingly, upon weakening of the cell wall, myosin rings in cps1-191 mutants expressing the regulatory light chain of myosin tagged with the fluorescent protein tdTomato (Rlc1-tdTomato) underwent contraction coupled with membrane ingression at the restrictive temperature of 36°C (Figure 2A; GFP-tagged Syntaxin-like protein Psy1 was used as a cell membrane marker; 19/29 spheroplasts). Consistently, contracting actin rings labeled with the Lifeact-mCherry were also detected in the cps1-191 mutant upon weakening of the cell wall,

suggesting that the actomyosin rings were driving the contraction and membrane ingression (Figure 2B; 5/41 spheroplasts). These mutant spheroplasts with weakened cell walls often divided nonmedially into two, and the rings contracted at much reduced rates (0.061 ± 0.021 μm/min; $n_{spheroplast}$ = 8) compared with wild-type cells (0.299 ± 0.059 μm/min; n_{cell} = 14; Figure 2C). The low rate of ring contraction is comparable to that in the wild-type spheroplasts, in which the rings slide along the cell membrane during ring contraction (0.046 ± 0.031 μm/min; $n_{wild-type\ spheroplast}$ = 40). We frequently observed that the rings contracted till midphase of division and disassembled before completion of cytokinesis. The spheroplasts, however, went on to divide into two entities (Figure 2, A and B). The segregation of daughter nuclei in the cps1-191 spheroplasts was often not coordinated with the cytokinesis, with some spheroplasts having two nuclei in one of the daughter entities or having cleaved nuclei, presumably due to the nonmedial division (Supplemental Figure 1). The miscoordination of cytofission and nuclear division spatially could arise from the variable dumbbell-shaped morphology of cps1-191 spheroplasts (Mishra et al., 2012). The functions of Mto1 and Mto2, which are involved in the assembly of postanaphase microtubule arrays, may also contribute to these miscoordination defects (Dundon and Pollard, 2020). Because the cps1-191 mutant spheroplast division was morphologically different from normal fission yeast cell division and was mimicking the morphological changes of some animal cells during division, we have called this type of division cytofission.

Analysis of the extracellular glycan matrix using calcofluor staining (a division septum–specific fluorochrome; G. Cortés et al., 2018) in cells undergoing cytofission in EMMA containing sorbitol and 2-DG medium revealed that the division site of cps1-191 spheroplasts undergoing cytofission with 2-DG medium contained significantly reduced β-glucan materials (Figure 2D). Further study with high-resolution scanning electron microscopy showed that the glucan fibrils regenerated in cps1-191 spheroplasts without 2-DG (Figure 2E, Bottom) while the fibrils were not noticeable in cps1-191 spheroplasts with 2-DG (Figure 2E, Top). The glucan fibrils commonly present at the division site of fission yeast were largely absent in cps1-191 spheroplasts undergoing cytofission (Supplemental Figure 2). Taking these results together, we showed that weakening of cell walls in cps1-191 cells at nonpermissive temperature and ensuing further inhibition of new cell wall and septum synthesis with 2-DG facilitate a novel cytofission event that leads to division of one spheroplast into two in the absence of detectable division-septum growth. Our results also suggested that the extracellular glycan matrix anchored to the actomyosin rings negatively regulates ring contraction and membrane ingression. This is consistent with a previous finding that the absence of Bgs4-synthesized β-glucan in the septum promoted faster ring contraction and membrane ingression than that of normal septa, and at the same time, the synthesis and ingression of septum wall progressed more slowly than that of a normal septum (Munoz et al., 2013).

A reduction of β-glucan may result in an increased amount of α-glucan in the cell walls of fission yeast. To test if the cytofission of cps1-191 spheroplasts was due to the synthesis of α-glucan at the division site, we prepared, cps1-191 mok1-664 double-mutant spheroplasts containing the thermosensitive alleles of both α- and β-glucan synthases and imaged the myosin rings and cell membranes in these double mutant spheroplasts at the nonpermissive temperature. Similar to the cps1-191 spheroplast, the cps1-191 mok1-664 double-mutant spheroplasts underwent cytofission (Figure 3A, 11/26), suggesting that α-glucan and β-glucan synthesis did not contribute significantly to the cytofission events.
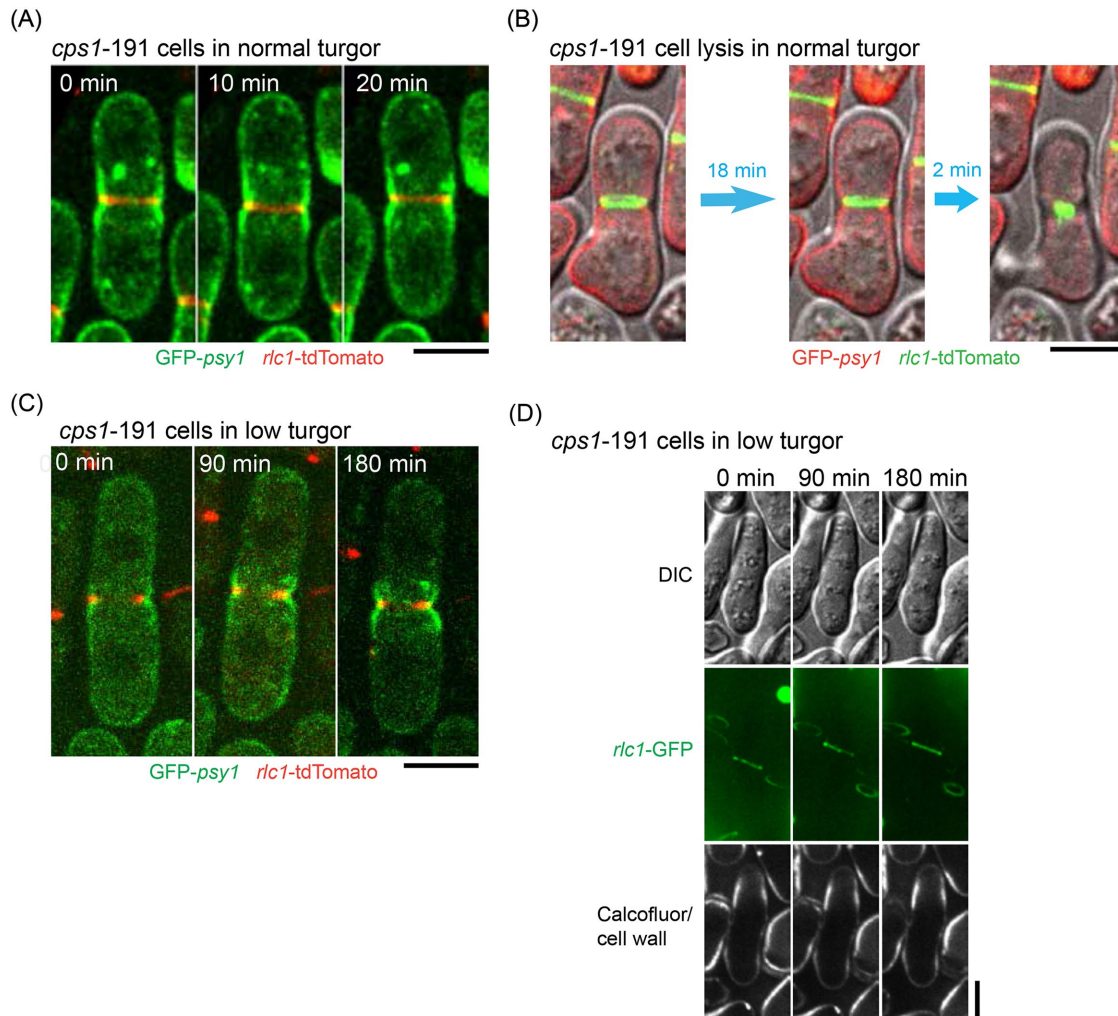
FIGURE 1: Lowering turgor pressure prevents cell membrane ingression in *cps1* mutant cells. (A) *cps1*-191 GFP-*psy1* *rlc1*-tdTomato cells were cultured in YEA at the restrictive temperature of 36°C for 6.5 h and were processed similarly using the spheroplasting protocol but omitting lysing enzymes and Zymolyase. Cells in the EMMA medium with 2-DG were imaged at 36°C. Green: GFP-*psy1*. Red: *rlc1*-tdTomato. (B) Some *cps1*-191 GFP-*psy1* *rlc1*-tdTomato cells lysed after more than 6.5 h of incubation at the restrictive temperature. Treatment of cells was the same as in A. Green: *rlc1*-tdTomato. Red: GFP-*psy1*. (C) *cps1*-191 GFP-*psy1* *rlc1*-tdTomato cells were cultured in YEA at the restrictive temperature for 6.5 h and were processed similarly using the spheroplasting protocol but omitting lysing enzymes and Zymolyase. Cells were imaged at 36°C in the EMMA medium containing 2-DG and 0.8 M sorbitol to lower down the turgor pressure. Green: GFP-*psy1*. Red: *rlc1*-tdTomato. (D) *cps1*-191 GFP-*psy1* *rlc1*-tdTomato cells treated as in C were stained with calcofluor dye to reveal the cell wall. Scale bar: 5 μm

Normal fission yeast cells that just complete ring contraction and membrane ingression are not entirely separated until the primary septum digestion of the division septum connecting the two newly divided cells (Sipiczki, 2007). This process is achieved in fission yeast through the action of endoglucanases (Martin-Cuadrado *et al.*, 2003; Dekker *et al.*, 2004; Garcia *et al.*, 2005). We tested if proteins involved in the separation of fission yeast cells were also involved in the cytofission, which would be expected if trace amounts of division septum had been deposited during ring contraction. To this end, we constructed double-mutant spheroplasts of *cps1*-191 lacking the endoglucanases *eng1* (β-glucanase) and *agn1* (α-glucanase), respectively. Similarly to the single mutant *cps1*-191, the double mutants lacking either of the two endoglucanases underwent cytofission upon weakening of the cell wall (Figure 3B, 8/23; Figure 3C, 11/38). The results indicated that the cytofission events of *cps1*-191 mutants do not require the breakdown of cell wall materials by en-

doglucanases, even though cytofission leads to the complete separation of spheroplasts.

In ~53% of the *cps1*-191 spheroplasts that underwent cytofission (53 out of 99 spheroplasts), the rings contracted till midphase of division and disassembled before division into two entities. We tested if the ESCRT abscission complex was involved in the cytofission by removing two of the ESCRT proteins Vps4 and Vps20 in the *cps1*-191 spheroplasts. The *cps1*-191 *vps4Δ* and *cps1*-191 *vps20Δ* double-mutant spheroplasts underwent cytofission as in the single *cps1*-191 mutant spheroplast (Supplemental Figure 3A, 14/14; Supplemental Figure 3B, 8/8). It is possible that the completion of cytofission without the actomyosin rings was achieved via an unknown cell abscission mechanism.

Previous studies suggested that in certain circumstances, some eukaryotic cells are able to divide without an actomyosin ring (Proctor *et al.*, 2012; Choudhary *et al.*, 2013; Flor-Parra *et al.*, 2014;

Dix et al., 2018; Ramos et al., 2019). To see if the cytofission was driven by contraction of the actomyosin ring, we first perturbed the functions of rings using Latrunculin-A (LatA) to inhibit actin polymerization (Morton et al., 2000; Fujiwara et al., 2018). cps1-191 spheroplasts treated with DMSO underwent ring contraction and membrane ingression and completed cytofission (Figure 4A; 11/16 spheroplasts). In contrast, cps1-191 spheroplasts treated with LatA underwent ring disassembly and failed to divide into two entities or ingressed very slowly, resembling dividing cells after long incubation with LatA (Ramos et al., 2019). Interestingly, the smaller entity retracted into the bigger entity, probably due to the imbalance of intracellular pressures (Figure 4B; 27/33 spheroplasts).

Next, we perturbed the myosin component of actomyosin rings by deleting rlc1, the regulatory light chain of myosin II (Le Goff et al., 2000; Naqvi et al., 2000; Pollard et al., 2017), in cps1-191 mutants. It has been shown that the cells lacking rlc1 (rlc1Δ) are cold-sensitive and fail to undergo cytokinesis at low temperatures, but at high temperatures, the rlc1Δ cells assemble an intact actomyosin ring that contracts normally (Naqvi et al., 2000; Supplemental Figure 4; 31/31 cells). We used this differential temperature requirement to test the essentiality of actomyosin ring functions in cytofission. If the actomyosin ring was essential in driving cytofission, the absence of rlc1 might render the cells with weakened cell walls unable to undergo cytofission at high temperatures, which are normally permissive for cell division in rlc1Δ cells alone (Naqvi et al., 2000). Consistent with the LatA experimental findings, the double mutant cps1-191 rlc1Δ with weakened cell walls did not undergo ring contraction at a high temperature (Figure 4C; 23/24 spheroplasts), whereas the single mutant of cps1-191 could undergo cytofission.

Targeted membrane deposition is required in the cytokinesis of fission yeast (Wang et al., 2016; Onwubiko et al., 2019). Next, we tested if targeted membrane deposition at the division site facilitates actomyosin ring contraction in cytofission. When the vesicular trafficking across the endomembrane system was inhibited using brefeldin A in the cps1-191 spheroplasts, the myosin rings were not able to contract to drive cytofission events (Figure 4D, 27/27). This result suggested that addition of cell membrane via targeted membrane trafficking at the division site is necessary to enable cytofission.

Our study reveals that the extracellular glycan matrix inhibits actomyosin ring contraction in the absence of cell wall remodeling and division septum synthesis. When the inhibition is relieved by experimental treatments such as ones reported in this study, or by septum synthesis, the actomyosin ring contracts to drive the membrane ingression. A previous study by Proctor et al. (2012) analyzed cps1-191 mutants and explained that the failure of membrane ingression in the mutant was due to a defect in division–septum assembly. The authors also proposed that the high intracellular turgor pressure prevents actomyosin ring contraction in fission yeast. We tested this model by lowering the turgor pressure in cps1-191 mutant cells and found that it was not sufficient to enable membrane ingression in the absence of cell wall remodeling in the cps1-191 cells. However, the ability of cps1-191 mutant cells to divide upon weakening of the cell wall indicates that the actomyosin ring in cps1-191 mutant cells is capable of driving membrane ingression even when the division-septum assembly is defective. When cell wall remodeling is normal, as in wild-type cells, ring contraction and membrane ingression coordinate with cell wall and septum growth. The lowering of turgor pressure by sorbitol addition in wild-type cells with normal cell wall remodeling may facilitate ring contraction, explaining the findings of Proctor et al (Proctor et al., 2012). The fact that ring contraction is slower during cytofission however, agrees better with the work of

O'Shaughnessy and colleagues, who have proposed that the rate of septum synthesis sets the rate of cytokinesis (Stachowiak et al., 2014). It is possible that our work reveals the highest rate of actomyosin ring contraction when confronted with membrane drag and viscous drag of the cytosol. The low ring contraction rate could be as a result of a reduced amount of Cps1-191 or cytokinetic proteins at the division site (Cortes et al., 2015). In fission yeast spheroplasts, the actomyosin ring is probably required at the early phase of cytofission to drive spheroplasts into a dumbbell shape with high curvature. Although we cannot exclude the possibility that residual and undetectable actomyosin structures may facilitate division after seeming actomyosin ring disassembly, recent work suggests other potential mechanisms not involving actomyosin rings or ESCRT in division of dumbbell-shaped vesicles. It has been proposed that the spontaneous curvature in dumbbell-shaped lipid vesicles generates constriction forces to induce membrane fission. This leads to the division of a dumbbell-shaped lipid vesicle into two with increased curvature (Steinkuhler et al., 2020).

The yeast cell wall consists mainly of glycan matrix and glycosylated proteins and has been suggested as a functional equivalent of the extracellular matrix (ECM) in animal cells (Munoz et al., 2013). The mechanical interaction between the cytokinetic actomyosin ring and the ECM is not well understood. A recent study of zebrafish epicardial cells in the heart explants shows the cell–ECM adhesions at the division site. The cell–ECM adhesions lead to the traction forces at the cytokinetic ring that inhibit cytokinesis (Uroz et al., 2019). An early biophysical study also detected a large traction force at the cleavage furrow of fibroblast cells cultured on an elastic substrate, suggesting an interaction of cytokinetic machinery and ECM (Burton and Taylor, 1997). When cell–ECM adhesion is enhanced during mitosis, cleavage furrow ingression is inhibited in the epithelial cells (Taneja et al., 2016). Consistently, our study shows that the anchoring to the extracellular glycan matrix of actomyosin rings that do not undergo remodeling (due to a defective Bgs1) prevents actomyosin ring contraction and cell membrane ingression. Weakening of the extracellular glycan matrix, presumably mimicking decreased cell–ECM adhesion, has enabled cytofission events.

MATERIALS AND METHODS
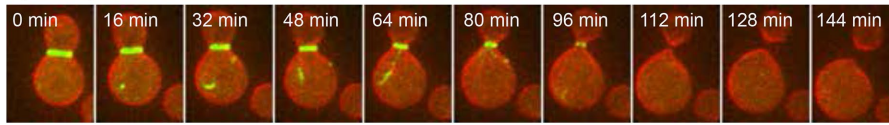
Yeast strains, media, and culture conditions
Table S1 lists the S. pombe strains used in our study. Standard fission yeast genetic techniques were used to prepare the strains. The rich medium YEA (5 g/l yeast extract, 30 g/l glucose, 225 mg/l adenine) was used to culture cells until midlog phase at 24°C before the temperature shift. LatA (Enzo Life Sciences; BML-T119) was used at a final concentration of 150 μM to perturb the actin dynamics in spheroplasts. Brefeldin A (Fisher Scientific; 15526276) was used at a final concentration of 75 μM to slow plasma membrane invagination. Calcofluor White Stain for cell wall staining was purchased from Sigma.

Preparation of Schizosaccharomyces pombe spheroplasts for live-cell imaging (spheroplasting)
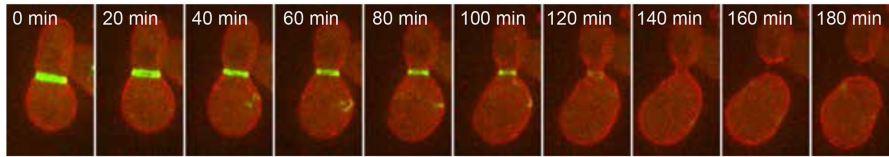The cps1-191 cells used in this study were first cultured in YEA medium at 24°C to midlog phase (OD_{595} = 0.2–0.5), and then were shifted to 36°C for 6 h 15 min (nonpermissive conditions). Twenty milliliters of culture were spun down at 3000 rpm for 1 min and washed once with an equal volume of E-buffer (50 mM sodium citrate, 100 mM sodium phosphate, pH 6.0). After the cells were spun down and resuspended in 5 ml of E-buffer containing 1.2 M sorbitol, the cell suspension was incubated with 30 mg of lysing enzymes from Trichoderma harzianum or Glucanex (Sigma, L1412; an
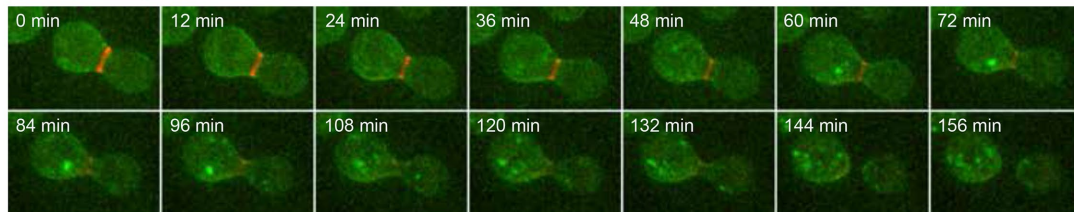
FIGURE 2: Weakening of cell walls allows ring contraction and cell membrane ingression. (A) Two examples of *cps1*-191 spheroplasts underwent cytofission at 36°C. The *cps1*-191 GFP-*psy1 rlc1*-tdTomato cells were cultured at 36°C for 6.5 h, processed into spheroplasts, and recovered for 1 h at 36°C before imaging. (B) Two examples of *cps1*-191 spheroplasts expressing Lifeact-mCherry underwent cytofission at 36°C. The *cps1*-191 GFP-*psy1 lifeact*-mCherry cells were cultured at 36°C for 6.5 h, processed into spheroplasts, and recovered for 1 h at 36°C before imaging. (C) Quantification of the rate of ring contraction in wild-type cells and *cps1*-191 spheroplasts undergoing cytofission. (D) Wild-type cells and
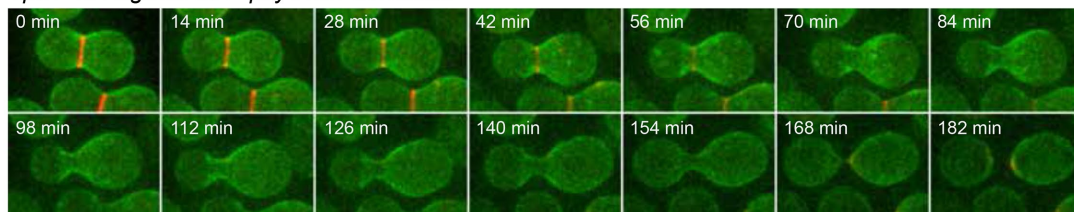
(A) *cps1*-191 *mok1*-664 GFP-*psy1 rlc1*-tdTomato

GFP-*psy1*   *rlc1*-tdTomato

(B) *cps1*-191 *eng1*Δ GFP-*psy1 rlc1*-tdTomato
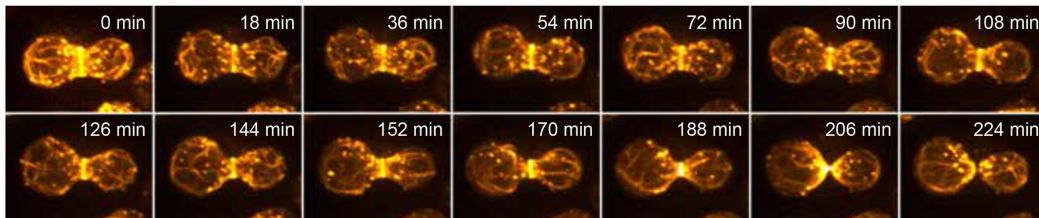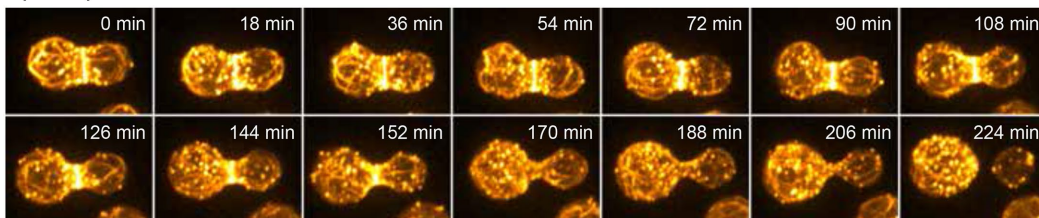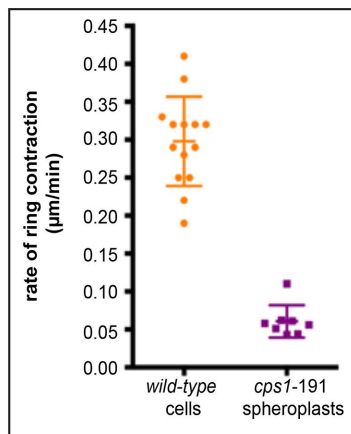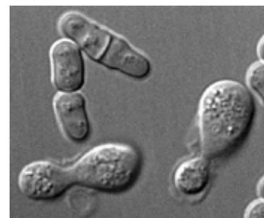
GFP-*psy1*   *rlc1*-tdTomato
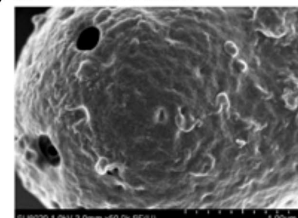
(C) *cps1*-191 *agn1*Δ GFP-*psy1 rlc1*-tdTomato
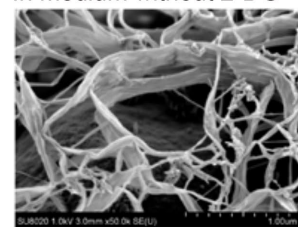
GFP-*psy1*   *rlc1*-tdTomato

FIGURE 3: The *cps1*-191 mutant spheroplasts undergo cytofission independent of the α-glucan synthase and endoglucanases. (A) Cytofission in *cps1*-191 *mok1*-664 GFP-*psy1 rlc1*-tdTomato. (B) Cytofission in *cps1*-191 *agn1*Δ GFP-*psy1 rlc1*-tdTomato. (C) Cytofission in *cps1*-191 *eng1*Δ GFP-*psy1 rlc1*-tdTomato. Scale bar: 5 μm.

enzymatic mixture with at least glucanase, cellulase, protease, and chitinase activities) at 36°C with shaking at 80 rpm for 90 min. This was followed by continuous incubation with 40 μl of LongLife Zymolyase (G-Biosciences, 1.5 U/μl; an enzymatic mixture with at least β-glucanase, protease, and mannanase activities) at 36°C with shaking at 80 rpm for 60 min. After enzymatic digestion, the cell suspensions were spun down at $450 \times g$ for 2 min and washed once with 5 ml of E-buffer containing 0.6 M sorbitol. After being spun at $450 \times g$ for 2 min, the spheroplasts were recovered in 10 ml EMMA (Edinburgh minimal medium with all amino acid and nucleotide supplements) containing 0.8 M sorbitol and 0.5% (vol/vol) of 1 M 2-deoxyglucose (Sigma, D6134) for 30 min at 36°C before microscopy imaging.

Sample preparation for light microscopy
One to two milliliters of spheroplast suspensions in EMMA containing 0.8 M sorbitol and 0.5% (vol/vol) of 1 M 2-deoxyglucose (Sigma, D6134) were concentrated to 20–100 μl by centrifugation at $450 \times g$ for 2 min. About 10 μl of concentrated spheroplasts were loaded onto an Ibidi μ-Slide 8-well glass-bottomed dish (Cat. No. 80827), and covered with mineral oil (Sigma, M5310) to prevent evaporation during the imaging process.

To image cells in Figure 1 and Supplemental Figure 4, the *cps1*-191 cells and *rlc1*Δ cells after shifting to nonpermissive conditions

were treated with buffers used to prepare spheroplasts, but with the lysing and lytic enzymes omitted to preserve the cell wall integrity. After the buffer washing, the *cps1*-191 cells in Figure 1 were recovered in EMMA with full supplements containing 0.8 M sorbitol and 0.5% 2-DG. For the *rlc1*Δ cells in the Supplemental Figure 4, after the buffer washing, the cells were recovered in EMMA with full supplements containing 0.8 M sorbitol but not 2-DG to allow septation.

### Sample preparation for electron microscopy
Two hundred fifty milliliters of cells with OD_{595} 0.2 were collected for spheroplasting. Spheroplasts were prepared by the spheroplasting method described above. Spheroplasts were spun down from EMMA with 0.8 M sorbitol and resuspended in phosphate-buffered saline (PBS) with 2.5% glutaraldehyde and 1.2 M sorbitol. Fixation solution was prepared by adding 2% glutaraldehyde and dissolving 1.2 M sorbitol in PBS. After 2 h incubation at room temperature, spheroplasts were spun down in round-bottomed tubes. The following procedures were done at 4°C and gently (vortex mixer was avoided). Spheroplasts were resuspended in fixation solution and stood on ice for 2 h. The spheroplasts were separated into 2 tubes: washed and unwashed samples. Unwashed samples were stored at 4°C. The washed samples were washed three times with 1 ml PBS

---

cps1-191 GFP-*psy1 rlc1*-tdTomato spheroplasts were stained with the dye calcofluor. The image was pseudo-colored in green to represent calcofluor staining. (E) Electron micrographs of *cps1*-191 GFP-*psy1 rlc1*-tdTomato spheroplasts regenerated in medium with or without 2-DG. Scale bar: 5 μm except E, which is 1 μm; error bars: SD.
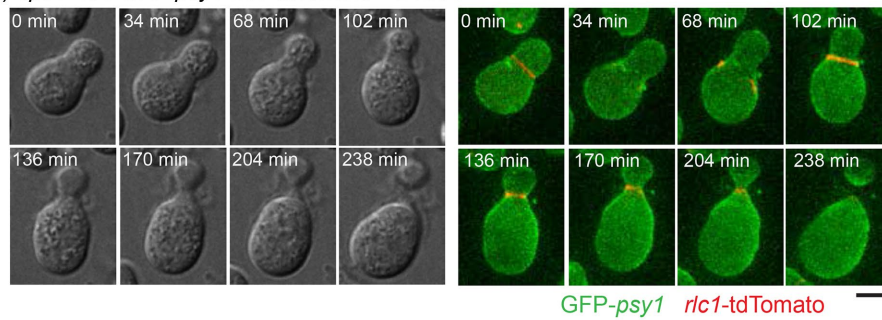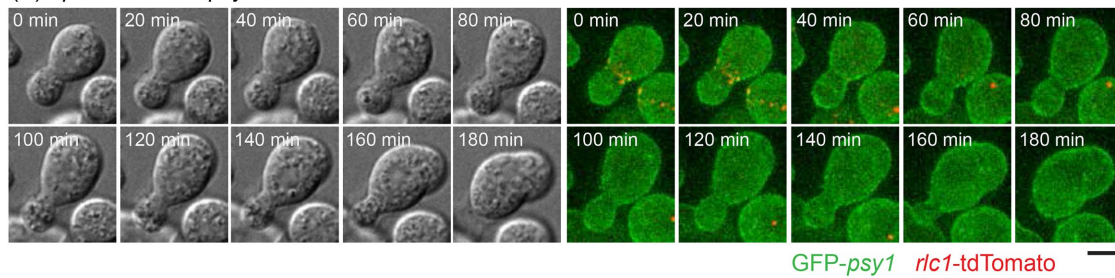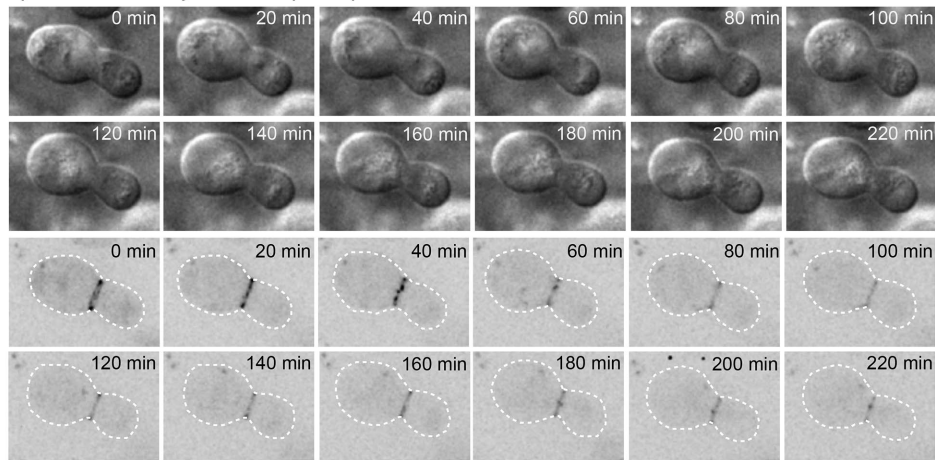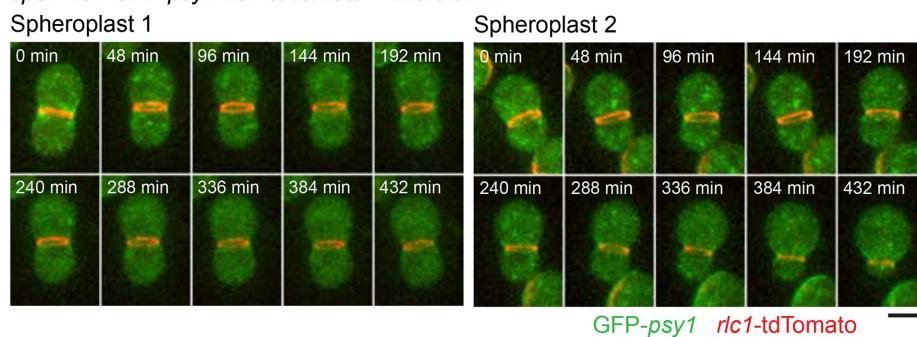
FIGURE 4: The function of actomyosin rings is required for the *cps1*-191 mutant spheroplasts to undergo cytofission. (A) *cps1*-191 GFP-*psy1* *rlc1*-tdTomato spheroplasts underwent cytofission in the presence of DMSO. Left panel shows the DIC images; Right panel shows the fluorescence micrographs. (B) *cps1*-191 GFP-*psy1* *rlc1*-tdTomato spheroplasts were incubated with 150 μm Lat-A. Left panel shows the DIC images; Right panel shows the fluorescence micrographs. (C) *rlc1*Δ *cyk3*-GFP spheroplasts failed to undergo cytofission at 36°C. The *rlc1*Δ *cyk3*-GFP cells were cultured at 36°C for 6.5 h, processed into spheroplasts, and then recovered in minimal medium containing sorbitol before imaging at 36°C. Top panel shows the DIC images; Bottom panel shows the fluorescence micrographs. (D) The *cps1*-191 GFP-*psy1* *rlc1*-tdTomato spheroplasts failed to undergo cytofission in the presence of 75 μM brefeldin A. Scale bar: 5 μm.

containing 1.2 M sorbitol. Last, the spheroplasts were resuspended in 1 ml PBS containing 1.2 M sorbitol and stored at 4°C before electron microscopy.

For electron microscopy, glutaraldehyde-fixed cells were placed on a slide glass whose surface was pretreated with 0.1% poly-L-lysine. They were washed with 0.1 M phosphate buffer (pH 7.2), postfixed with 1% osmium tetroxide at 4°C for 1 h, dehydrated with graded series of ethanol, and critical point–dried with a Leica EM CPD030 apparatus (Leica Microsystems, Vienna). The specimens were coated with osmium tetroxide by an osmium coater (Vacuum Device, Japan) and observed with S-3400N and SU8020 scanning electron microscopes (Hitachi High Technologies, Tokyo) at 10.0 kV and 1.0 kV, respectively (Namiki *et al.*, 2011).

Light microscopy

An Andor Revolution XD spinning disk confocal microscope was used to image the spheroplasts and cells at 36°C. The microscope was equipped with a Nikon ECLIPSE Ti inverted microscope, a Nikon Plan Apo Lambda 100 ×/1.45N.A. oil immersion objective lens, a spinning-disk system (CSU-X1; Yokogawa), and an Andor iXon Ultra EMCCD camera 897 or 888. Andor IQ3 software was used to acquire images at a pixel size of 80 or 69 nm/pixel, depending on the camera model. Laser lines at wavelengths of 405, 488, or 561 nm were used for the excitation of fluorophores. Most images were acquired with Z-step sizes of 0.5 μm as listed here: Figure 2A (12 μm/25 Z-sections); Figure 2B (10 μm/21 Z-sections); Figure 3A (10 μm/21 Z-sections); Figure 3B (15 μm/31 Z-sections); Figure 3C (15 μm/31 Z-sections); Figure 4A (15 μm/31 Z-sections); Figure 4B (12 μm/25 Z-sections); Figure 4C (13 μm/27 Z-sections); Figure 4D (10 μm/21 Z-sections); Supplemental Figure 1 (10 μm/21 Z-sections); Supplemental Figure 3A (15 μm/31 Z-sections); Supplemental Figure 3B (13 μm/27 Z-sections); Supplemental Figure 4 (13 μm/27 Z-sections).

Image analysis

Images were processed using Fiji. The time-lapse montages are maximum-intensity projections of Z-stacks of specified time points. All images analyzed were prepared in this study, except images for quantification of the rate of ring sliding in wild-type spheroplasts, in which the data were based on time-lapse images acquired in a previous study (Lim *et al.*, 2018).

REFERENCES

Arasada R, Pollard TD (2014). Contractile ring stability in *S. pombe* depends on F-BAR protein Cdc15p and Bgs1p transport from the Golgi complex. Cell Rep 8, 1533–1544.

Arasada R, Pollard TD (2015). A role for F-BAR protein Rga7p during cytokinesis in S. pombe. J Cell Sci 128, 2259–2268.

Burton K, Taylor DL (1997). Traction forces of cytokinesis measured with optically modified elastic substrata. Nature 385, 450–454.

Choudhary A, Lera RF, Martowicz ML, Oxendine K, Laffin JJ, Weaver BA, Burkard ME (2013). Interphase cytofission maintains genomic integrity of human cells after failed cytokinesis. Proc Natl Acad Sci USA 110, 13026–13031.

Cortes JC, Carnero E, Ishiguro J, Sanchez Y, Duran A, Ribas JC (2005). The novel fission yeast (1,3)beta-D-glucan synthase catalytic subunit Bgs4p is essential during both cytokinesis and polarized growth. J Cell Sci 118, 157–174.

Cortes JC, Pujol N, Sato M, Pinar M, Ramos M, Moreno B, Osumi M, Ribas JC, Perez P (2015). Cooperation between paxillin-like protein Pxl1 and glucan synthase Bgs1 is essential for actomyosin ring stability and septum formation in fission yeast. PLoS Genet 11, e1005358.

Cortes JC, Sato M, Munoz J, Moreno MB, Clemente-Ramos JA, Ramos M, Okada H, Osumi M, Duran A, Ribas JC (2012). Fission yeast Ags1 confers the essential septum strength needed for safe gradual cell abscission. J Cell Biol 198, 637–656.

Davidson R, Pontasch JA, Wu JQ (2016). Sbg1 is a novel regulator for the localization of the beta-glucan synthase Bgs1 in fission yeast. PLoS One 11, e0167043.

Dekker N, Speijer D, Grun CH, van den Berg M, de Haan A, Hochstenbach F (2004). Role of the alpha-glucanase Agn1p in fission-yeast cell separation. Mol Biol Cell 15, 3903–3914.

Dix CL, Matthews HK, Uroz M, McLaren S, Wolf L, Heatley N, Win Z, Almada P, Henriques R, Boutros M, *et al.* (2018). The role of mitotic cell–substrate adhesion re-modeling in animal cell division. Dev Cell 45, 132–145.e133.

Dundon SER, Pollard TD (2020). Microtubule nucleation promoters Mto1 and Mto2 regulate cytokinesis in fission yeast. Mol Biol Cell mbcE19120686.

Flor-Parra I, Bernal M, Zhurinsky J, Daga RR (2014). Cell migration and division in amoeboid-like fission yeast. Biol Open 3, 108–115.

Fujiwara I, Zweifel ME, Courtemanche N, Pollard TD (2018). Latrunculin A accelerates actin filament depolymerization in addition to sequestering actin monomers. Curr Biol 28, 3183–3192.e3182.

Garcia Cortes JC, Ramos M, Osumi M, Perez P, Ribas JC (2016). The cell biology of fission yeast septation. Microbiol Mol Biol Rev 80, 779–791.

Garcia I, Jimenez D, Martin V, Duran A, Sanchez Y (2005). The alpha-glucanase Agn1p is required for cell separation in *Schizosaccharomyces pombe*. Biol Cell 97, 569–576.

G. Cortés JC, Ramos M, Konomi M, Barragan I, Moreno MB, Alcaide-Gavilan M, Moreno S, Osumi M, Perez P, Ribas JC (2018). Specific detection of fission yeast primary septum reveals septum and cleavage furrow ingression during early anaphase independent of mitosis completion. PLoS Genet 14, e1007388.

Le Goff X, Motegi F, Salimova E, Mabuchi I, Simanis V (2000). The *S. pombe* rlc1 gene encodes a putative myosin regulatory light chain that binds the type II myosins myo3p and myo2p. J Cell Sci 113 (Pt 23), 4157–4163.

Lim TC, Hatano T, Kamnev A, Balasubramanian MK, Chew TG (2018). Equatorial assembly of the cell-division actomyosin ring in the absence of cytokinetic spatial cues. Curr Biol 28, 955–962.e953.

Liu J, Wang H, Balasubramanian MK (2000). A checkpoint that monitors cytokinesis in *Schizosaccharomyces pombe*. J Cell Sci 113 (Pt 7), 1223–1230.

Martin-Cuadrado AB, Duenas E, Sipiczki M, Vazquez de Aldana CR, del Rey F (2003). The endo-beta-1,3-glucanase eng1p is required for dissolution of the primary septum during cell separation in *Schizosaccharomyces pombe*. J Cell Sci 116, 1689–1698.

Martin-Garcia R, Arribas V, Coll PM, Pinar M, Viana RA, Rincon SA, Correa-Bordes J, Ribas JC, Perez P (2018). Paxillin-mediated recruitment of calcineurin to the contractile ring is required for the correct progression of cytokinesis in fission yeast. Cell Rep 25, 772–783.e774.

Megnet R (1965). Effect of 2-deoxyglucose on *Schizosaccharomyces pombe*. J Bacteriol 90, 1032–1035.

Mishra M, Huang Y, Srivastava P, Srinivasan R, Sevugan M, Shlomovitz R, Gov N, Rao M, Balasubramanian M (2012). Cylindrical cellular geometry ensures fidelity of division site placement in fission yeast. J Cell Sci 125, 3850–3857.

Morton WM, Ayscough KR, McLaughlin PJ (2000). Latrunculin alters the actin-monomer subunit interface to prevent polymerization. Nat Cell Biol 2, 376–378.

Munoz J, Cortes JC, Sipiczki M, Ramos M, Clemente-Ramos JA, Moreno MB, Martins IM, Perez P, Ribas JC (2013). Extracellular cell wall beta(1,3) glucan is required to couple septation to actomyosin ring contraction. J Cell Biol 203, 265–282.

Namiki Y, Ueno K, Mitani H, Virtudazo EV, Ohkusu M, Shimizu K, Kawamoto S, Chibana H, Yamaguchi M (2011). Scanning and negative-staining electron microscopy of protoplast regeneration of a wild-type and two chitin synthase mutants in the pathogenic yeast Candida glabrata. J Electron Microsc (Tokyo) 60, 157–165.

Naqvi NI, Wong KC, Tang X, Balasubramanian MK (2000). Type II myosin regulatory light chain relieves auto-inhibition of myosin-heavy-chain function. Nat Cell Biol 2, 855–858.

Onwubiko UN, Mlynarczyk PJ, Wei B, Habiyaremye J, Clack A, Abel SM, Das ME (2019). A Cdc42 GEF, Gef1, through endocytosis organizes F-BAR Cdc15 along the actomyosin ring and promotes concentric furrowing. J Cell Sci 132.

Osumi M, Sato M, Ishijima SA, Konomi M, Takagi T, Yaguchi H (1998). Dynamics of cell wall formation in fission yeast, *Schizosaccharomyces pombe*. Fungal Genet Biol 24, 178–206.

Pollard LW, Bookwalter CS, Tang Q, Krementsova EB, Trybus KM, Lowey S (2017). Fission yeast myosin Myo2 is down-regulated in actin affinity by light chain phosphorylation. Proc Natl Acad Sci USA 114, E7236–E7244.

Proctor SA, Minc N, Boudaoud A, Chang F (2012). Contributions of turgor pressure, the contractile ring, and septum assembly to forces in cytokinesis in fission yeast. Curr Biol 22, 1601–1608.

Ramos M, Cortes JCG, Sato M, Rincon SA, Moreno MB, Clemente-Ramos JA, Osumi M, Perez P, Ribas JC (2019). Two *S. pombe* septation phases differ in ingression rate, septum structure, and response to F-actin loss. J Cell Biol 218, 4171–4194.

Sethi K, Palani S, Cortes JC, Sato M, Sevugan M, Ramos M, Vijaykumar S, Osumi M, Naqvi NI, Ribas JC, Balasubramanian M (2016). A new membrane protein Sbg1 links the contractile ring apparatus and septum synthesis machinery in fission yeast. PLoS Genet 12, e1006383.

Sipiczki M (2007). Splitting of the fission yeast septum. FEMS Yeast Res 7, 761–770.

Stachowiak MR, Laplante C, Chin HF, Guirao B, Karatekin E, Pollard TD, O'Shaughnessy B (2014). Mechanism of cytokinetic contractile ring constriction in fission yeast. Dev Cell 29, 547–561.

Steinkuhler J, Knorr RL, Zhao Z, Bhatia T, Bartelt SM, Wegner S, Dimova R, Lipowsky R (2020). Controlled division of cell-sized vesicles by low densities of membrane-bound proteins. Nat Commun 11, 905.

Svoboda A, Smith DG (1972). Inhibitory effect of 2-deoxy-glucose on cell wall synthesis in cells and protoplasts of *Schizosaccharomyces pombe*. Z Allg Mikrobiol 12, 685–699.

Taneja N, Fenix AM, Rathbun L, Millis BA, Tyska MJ, Hehnly H, Burnette DT (2016). Focal adhesions control cleavage furrow shape and spindle tilt during mitosis. Sci Rep 6, 29846.

Uroz M, Garcia-Puig A, Tekeli I, Elosegui-Artola A, Abenza JF, Marin-Llaurado A, Pujals S, Conte V, Albertazzi L, Roca-Cusachs P, *et al.* (2019). Traction forces at the cytokinetic ring regulate cell division and polyploidy in the migrating zebrafish epicardium. Nat Mater 18, 1015–1023.

Wang N, Lee IJ, Rask G, Wu JQ (2016). Roles of the TRAPP-II complex and the exocyst in membrane deposition during fission yeast cytokinesis. PLoS Biol 14, e1002437.